SLAC-PUB-13272
Revised – March 2009

TTF HOM DATA ANALYSIS WITH CURVE FITTING METHOD

S. Pei#, C. Adolphsen, Z. Li, K. Bane and J. Smith, SLAC, CA 94025

Abstract

To investigate the possibility of using HOM signals induced in SC cavities as beam and cavity diagnostics, narrow band (20 MHz) data was recorded around the strong TE111-6(6π/9-like) dipole modes (1.7 GHz) in the 40 L-band (1.3 GHz) cavities at the DESY TTF facility. The analyses of these data have so far focused on using a Singular Value Decomposition (SVD) technique to correlate the signals with each other and data from conventional BPMs to show the dipole signals provide an alternate means of measuring the beam trajectory. However, these analyses do not extract the modal information (i.e., frequencies and Q's of the nearly degenerate horizontal and vertical modes). In this paper, we described a method to fit the signal frequency spectrum to obtain this information, and then use the resulting mode amplitudes and phases together with conventional BPM data to determine the mode polarizations and relative centers and tilts. Compared with the SVD analysis, this method is more physical, and can also be used to obtain the beam position and trajectory angle.

INTRODUCTION

When charged particle beams traverse an accelerator cavity, the wakefield induced by the upstream bunches in a bunch train act on the downstream bunches, and may degrade the beam qualities. In the DESY TTF facility, the long-range transverse wakefield is damped by HOM couplers that are located on each end of the 9-cell SC cavities. By analyzing the coupler signals after they are processed/recorded with appropriate down-mix digitizing electronics, the modal frequencies, Q's and relative phases can be extracted. Using the resulting mode amplitudes together with conventional BPM data, the mode centers, tilts and polarizations can also be determined.

Analysis of 1.7 GHz narrow-band dipole data has been done successfully using a SVD technique, which doesn't require knowledge of the mode properties and the machine optics [1]. Here we present an analysis of the data that also determines the mode properties.

DIPOLE MODE RESPONSE

A dipole mode can be excited in a cavity in three generalized ways [2]: pure offset, pure trajectory angle and pure bunch tilt, which are illustrated in Fig. 1.

The amplitude of resulting coupler signal can be expressed as follows：

$$V_{offset}(t) \propto xe^{-t/2\tau}\sin(\omega t) \quad (1)$$

$$V_{tracjectory\_angle}(t) \propto \theta e^{-t/2\tau}\cos(\omega t) \quad (2)$$

$$V_{tilt\_angle}(t) \propto -\alpha e^{-t/2\tau}\cos(\omega t) \quad (3)$$

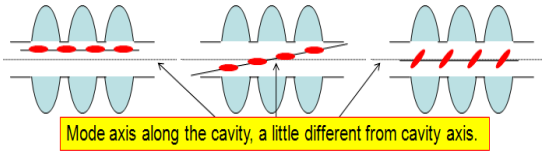

Fig. 1: Three ways to excite dipole modes.

The signal excited by pure offset (in-phase or IP) is 90° out-of-phase from that induced by pure trajectory angle and pure bunch tilt (out-of-phase or OP). Due to the very short bunch lengths (~50fs) in the TTF linac, the bunch tilt angle contribution can be ignored. Also, the bunch trajectory contribution is generally small (simulations show that the dipole mode amplitude induced by 1 mrad trajectory angle is about 10%-15% of that induced by 1 mm offset in the 1.0 m long SC cavities with fundamental mode and HOM mode couplers [3][4]: in our analysis, we assume 12%). Ignoring the mode Q's, the dipole signal can then be expressed as:

$$\begin{aligned} V_{HOM}(t) &= V_{offset}(t) + V_{trajectory\_angle}(t) + V_{tilt\_angle}(t) \\ &\approx V_{offset}(t) + V_{trajectory\_angle}(t) \\ &\approx \sqrt{(V_{offset\_amp})^2 + (V_{trajectory\_angle\_amp})^2}\cos(\omega_0 t + \varphi) \end{aligned} \quad (4)$$

Where $\varphi = \tan^{-1}(V_{trajectory\_angle\_amp}/V_{Offset\_amp})$. If there are many dipole modes, we have

$$V_{HOM}(t) = \sum_{n=1}^{\infty} A_n \cos(\omega_{0n} t + \varphi_n) \quad (5)$$

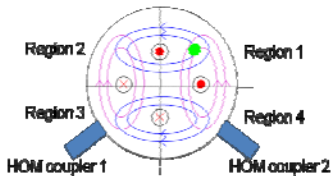

Fig. 2. Different dipole mode polarizations.

DIPOLE MODE PHASE

Dipole modes appear in pairs with different polarizations. The frequencies of these polarizations are nearly degenerate and are further split due to cell asymmetries and fabrication errors. In Fig.2, if the HOM signal is excited by a beam with a constant offset in region 1, for example, the phase difference of the two polarization signals will be 0° at HOM coupler 1 and 180° at HOM coupler 2 (assuming the two degenerate modes have almost same resonant frequency and the time after the dipole mode excitation is not too long). If the beam trajectory has some angle,

*Work supported by the DOE under Contract DE-AC02-76SF00515.
slpei@slac.stanford.edu

the phase difference will deviate from 0^o or 180^o. The down-mix cables may also affect the phase difference.

DATA ANALYSIS

Our curve fitting analysis can be divided into two basic steps. In the First Step Fitting (FSF), the dipole mode frequencies, Q's, amplitudes and relative phases are extracted, while in the Second Step Fitting (SSF), the dipole mode centers, polarization angles, cavity tilt angles and reference phases are extracted.

First Step Fitting

Considering the finite Q of the dipole mode, the HOM signal in the time domain can be expressed as,

$$\sum_{n=1}^{\infty} A_n \cos(\omega_{0n} t + \varphi_n)\exp(-\omega_{0n} t / 2Q_n) \quad (6)$$

The Fourier transform is a complex Lorentzian,

$$\sum_{n=1}^{\infty} A_n \frac{2Q_n(-2jQ_n\omega\cos(\varphi_n)+(-\cos(\varphi_n)+2Q_n\sin(\varphi_n))\omega_{0n})}{4Q_n^2\omega^2-\omega_{0n}(4jQ_n\omega+(1+4Q_n^2)\omega_{0n})} \quad (7)$$

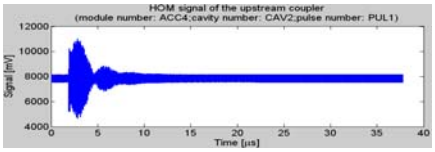

Fig. 3. Typical dipole signal.

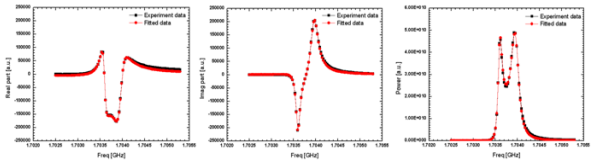

Fig. 4. Frequency domain fitting of the real part, imaginary part and the amplitude (from left to right)

Fig. 3 shows an example of the narrow-band dipole signal. The beating of the signal indicates the dipole mode polarizations are not degenerate. In order to eliminate the effect of the direct beam excitation, the early part of the waveform (before sample 300, same as in Ref. [1]) was not used. Fig. 4 shows an example of the frequency domain data fits to the complex Lorentzian function, Eq. (7), where the black curves are the data and the red curves are the fits.

Fig. 5 shows typical results for the dipole mode frequencies and Q's obtained from a data set of 36 pulses where the beam was moved transversely in one complete circle. For each pulse, data from both the upstream and downstream HOM couplers were analyzed separately to extract the two polarization frequencies and Q's. The variation of these results indicates the systematic errors, which depend on the sampling frequency and number of sampling points. It is several kHz for the frequency, and several hundred for the Q's.

Fig. 6 shows the dipole mode amplitudes for a set of 36 pulses that span a circle. Note the dipole mode centers (cross point of the two polarization axis) are far outside this circle. In order to reduce the systematic error, the fitting of the 36×2 signals was done for each cavity using a common mode frequency and Q for each coupler while the phase and amplitudes varied for each pulse/coupler. So 36×4+2+2=148 parameters were fit at the same time. In Fig. 6, the amplitude variation of the polarization mode 1 is sine-like while mode 2 is cosine-like, indicating that the polarizations are about 90 degrees apart azimuthally.

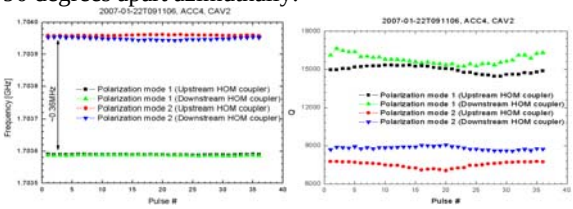

Fig. 5. Fit dipole mode frequencies and Q's (2^{nd} cavity of module 4 for dataset 2007-01-22T091106).

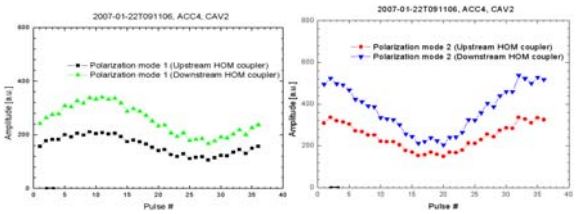

Fig. 6. Fit dipole mode amplitudes (2nd cavity of module 4 for dataset 2007-01-22T091106).

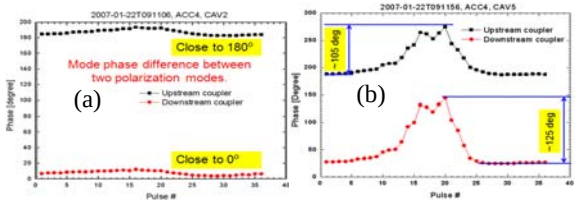

Fig. 7. Phase difference of the two polarization modes (2^{nd} and 5^{th} cavity of module 4 for 2007-01-22T091106).

Fig. 7(a) shows the phase difference of the two polarization modes for the 2^{nd} cavity in module 4, which is consistent with our expectation of 0^o and 180^o except for small variations (~10^o), which are probably caused by beam timing variations (possibly due to orbit effects in the two bunch compressors before this cavity). For other cavities in this data set, the beam passes closer to the mode center, and the phase variation is relatively large, indicating the existence of a finite OP component relative to the small IP component. Fig. 7(b) shows one example with a large phase variation. Fig. 8 shows the FSF analysis results for cavities in module 4 and module 5 for data set 2007-01-22T091106.

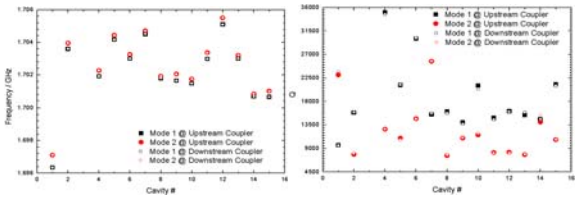

Fig. 8. FSF results for cavities in module 4 and 5.

Second Step Fitting

In the FSF analysis, the amplitude(A) and phases(φ) of modes are determined. The IP portion is proportional to the beam offset relative to the mode center while the OP portion is proportional to the beam trajectory angle relative to the mode axis in the cavity. For the SSF, these data are analyzed in terms of the BPM readings at the ends of each 8-cavity module. In particular, they are fit to the beam position in the BPM coordinate system at the start, middle and end of a specific cavity, which are obtained through linear interpolation. Also, the beam timing jitter($\Delta\varphi$) phase corrections are obtained by time domain analysis of the raw signal data. Using this information and the simulated normalized amplitude ratio ($A_{OP-norm}$ / $A_{IP-norm}$ =0.12mm/mrad) of the IP and OP components, the dipole mode center, polarization angle, cavity tilt angle and IP and OP normalized amplitudes are obtained.

The IP model used in SSF can be interpreted from Fig. 9(a) and Eq. (8), while the OP model can be interpreted from Fig. 9(b) and Eq. (9).

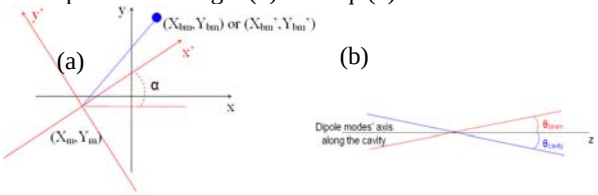

Fig. 9. Schematic of the IP and OP model.

$$A_{IP} = A\cos\left(\varphi - \varphi_{ref} + \Delta\varphi\right) = \begin{cases} A_{IP-norm}\sqrt{\left(X_{bm}-X_m\right)^2+\left(Y_{bm}-Y_m\right)^2} \\ \quad \times\sin\left(\tan^{-1}\left(\dfrac{Y_{bm}-Y_m}{X_{bm}-X_m}\right)-\alpha\right) & \left(X_{bm}-X_m\right)\geq 0 \\ A_{IP-norm}\sqrt{\left(X_{bm}-X_m\right)^2+\left(Y_{bm}-Y_m\right)^2} \\ \quad \times\sin\left(\tan^{-1}\left(\dfrac{Y_{bm}-Y_m}{X_{bm}-X_m}\right)+\pi-\alpha\right) & \left(X_{bm}-X_m\right)\leq 0 \end{cases} \quad (8)$$

$$A_{OP} = A\sin\left(\varphi - \varphi_{ref} + \Delta\varphi\right) = A_{OP-norm}\tan\left(\theta_{beam}-\theta_{cavity}\right) = A_{OP-norm}\tan\left(\tan^{-1}\left(\frac{Y'_{be}}{Y'_{bs}}\right)-\theta_{cavity}\right) = A_{OP-norm}\tan\left(\tan^{-1}\left(\frac{(Y_{be}-Y_{bs})\cos\alpha-(X_{be}-X_{bs})\sin\alpha}{L}\right)-\theta_{cavity}\right) \quad (9)$$

$\left(X_{bm},Y_{bm}\right)$ and $\left(X'_{bm},Y'_{bm}\right)$ are the beam position in the BPM coordinate system and dipole mode coordinate system. $\left(X_m,Y_m\right)$ is the dipole mode center in BPM coordinate system. $\left(X_{bs},Y_{bs}\right)$ and $\left(X_{be},Y_{be}\right)$ are the beam positions at the start and end of the cavity in the BPM coordinate system, while $\left(X'_{bs},Y'_{bs}\right)$ and $\left(X'_{be},Y'_{be}\right)$ are beam positions in dipole modes' coordinate system. φ_{ref} is the phase of the pure IP component, which is a constant and fit variable. Finally, α is the polarization angle and a fit variable. Table 1 lists the mode center and polarization analysis results for cavities in module 4 and 5 for data set 2007-01-22T091106.

CONCLUSIONS

It has been shown that a frequency domain fitting method can be used to extract dipole mode information, and that these results can then be used to determine relative mode polarizations, centers and tilts. The accuracy of this method depends on the external BPM system and the down-mix electronics. Beam timing variations of 10-15ps (peak to peak) were found, likely from bunch compressor effects. Further work is needed to more precisely eliminate the beam timing effects to be able to extract accurate cavity tilt information.

ACKNOWLEDGE

Thank S. Molloy and J. Frisch for helpful discussion.

REFERENCES

[1] S. Molloy et al., PRST-AB 9, 112802 (2006).
[2] S. Walston et al., NIM A 578 (2007) 1-22.
[3] Z. Li, Private Communication.
[4] K. L. Bane, Private Communication.

Table 1. Results of the SSF for cavities in module 4 and 5

Cavity #	Mode Center / mm	Mode Pol. / deg	Cavity #	Mode Center / mm	Mode-1 Pol. / deg
4-1	(-3.20, -1.09)	(-21.75, 69.51)	5-1	(-0.17, 0.23)	(14.01, 109.71)
4-2	(-2.73, -2.21)	(1.70, 93.32)	5-2	(0.23, -0.40)	(3.59, 94.63)
4-3			5-3	(0.86, -0.13)	(7.09, 99.17)

4-4	(-1.88, -1.59)	(20.90, 111.58)	5-4	(1.38, -0.82)	(5.59, 98.28)
4-5	(-1.34, -1.43)	(1.69, 93.20)	5-5	(0.72, -0.51)	(-5.35, 82.70)
4-6	(-1.09, -0.98)	(3.41, 94.15)	5-6	(0.68, -0.35)	(-54.23, 29.63)
4-7	(-0.18, -0.94)	(-15.79, 73.08)	5-7	(0.79, -0.65)	(-1.86, 87.02)
4-8	(-0.12, -0.36)	(-22.61, 68.97)	5-8		